Synthesis, in Vitro Metabolism, Cell Transformation, Mutagenicity, and DNA Adduction of Dibenzo[*c,mno*]chrysene

Dhimant Desai,*,† Arun K. Sharma,† Jyh-Ming Lin,† Jacek Krzeminski,† Maria Pimentel,‡ Karam El-Bayoumy,† Stephen Nesnow,‡ and Shantu Amin†

American Health Foundation, 1 Dana Road, Valhalla, New York 10595, and U. S. Environmental Protection Agency, ORD, MD-68, Research Triangle Park, North Carolina 27711

Received February 6, 2002

Polycyclic aromatic hydrocarbons (PAHs) are ubiquitous environmental pollutants. Due to its structural similarity with the potent carcinogen dibenzo[*a,l*]pyrene (DB[*a,l*]P) and because of its environmental presence, dibenzo[*c,mno*]chrysene (naphtho[1,2-*a*]pyrene, N[1,2-*a*]P) is of considerable research interest. We therefore developed an efficient synthesis of N[1,2-*a*]P, and examined its in vitro metabolism by male Sprague Dawley rat liver *S9* fraction. Its mutagenic activity in *S. typhimurium* TA 100 and its morphological cell transforming ability in mouse embryo fibroblasts were evaluated. On the basis of spectral analyses, the in vitro major metabolites were identified as the fjord region dihydrodiol *trans*-9,10-dihydroxy-9,10-dihydro-N[1,2-*a*]P (N[1,2-a]P-9,10-dihydrodiol), the K-region diols N[1,2-*a*]P-4,5-dihydrodiol and N[1,2-*a*]P-7,8-dihydrodiol, and also the 1-, 3-, and 10-hydroxy-N[1,2-*a*]P; the structure of N[1,2-*a*]P-9,10-dihydrodiol was also confirmed by independent synthesis. In assays with *S. typhimurium* TA 100, N[1,2-*a*]P-9,10-dihydrodiol was half as mutagenic as (±)-*trans*-7,8-dihydroxy-7,8-dihydrobenzo[*a*]pyrene (B[*a*]P-7,8-dihydrodiol) at ≥4 nmol/plate. N[1,2-*a*]P-9,-10-dihydrodiol was much more mutagenic than N[1,2-*a*]P at all dose levels, suggesting that the N[1,2-*a*]P-9,10-dihydrodiol is the likely proximate mutagen of N[1,2-*a*]P. Evaluation of morphological cell transformation in C3H10T1/2C18 mouse embryo fibroblasts revealed that N[1,2-*a*]P was comparable to B[*a*]P. We further examined the pattern of in vitro adduct formation between calf thymus DNA and (±)-*anti*-9,10-dihydroxy-9,10-dihydro-11,12-epoxy-9,10,11,12-tetrahydro-N[1,2-*a*]P (N[1,2-*a*]PDE) and found that dG-adduct formation is 2.9-fold greater than dA-adduct formation. On the basis of our results and those reported in the literature, our working hypothesis is that N[1,2-*a*]P may be added to the list of potent carcinogens that includes DB[*a,l*]P. This hypothesis is currently being tested in our laboratory.

Introduction

Polycyclic aromatic hydrocarbons (PAHs)[1] are environmental pollutants of widely varying structural composition. The genotoxicity of PAHs is strongly linked to their structural features. Dibenzo[*a,l*]pyrene (DB[*a,l*]P), a hexacyclic PAH with a pyrene moiety and a fjord region, has attracted much attention because of its unsurpassed mutagenicity and carcinogenicity (*1*−*5*). In both mutagenicity and carcinogenicity assays, DB[*a,l*]P is much more potent than benzo[*a*]pyrene (B[*a*]P) (*1*−*5*). It is logical, therefore, to investigate peri-condensed hexacyclic PAHs with a fjord region with respect to their genotoxicity. However, peri-condensed hexacyclic PAHs are a diverse group of compounds with 15 possible different structures, 12 of which have a pyrene moiety (*6*). On the basis of their environmental ubiquity and structural similarity with DB[*a,l*]P, some naphthopyrene (NP) isomers have been synthesized and tested; while N[2,1-*a*]P and N[2,3-*a*]P were moderately active carcinogens, N[2,3-*e*]P had no effect (*7*−*9*).

Out of 12 possible hexacyclic isomers of pyrene, 10 were known to be present in environmental samples (*9*); however, recent studies have also identified the remaining 2 isomers, N[1,2-*a*]P and naphtho[1,2-*e*]pyrene [N[1,2-*e*]P in coal tar extract, in air-borne particulate matter, and in marine sediment (Stephen Wise et al., unpublished results)]. We hypothesized that N[1,2-*a*]P and N[1,2-*e*]P are potent genotoxins because of their shared structural similarity with DB[*a,l*]P, namely, a pyrene moiety as well as a fjord region. To test this hypothesis, we have synthesized N[1,2-*a*]P and examined its in vitro metabolism with *S*9 fraction of phenobarbital/*β*-naphthoflavone-induced male Sprague Dawley rat liver homogenate. To gain insight into metabolic pathways of N[1,2-*a*]P that may lead to its genotoxicity, we evaluated the mutagenicity of N[1,2-*a*]P and of its terminal ring dihydrodiol toward *S. typhimurium* TA 100. The cytotoxicity and morphological cell transforming activity of N[1,2-*a*]P were also compared to B[*a*]P in C3H10T1/2 mouse embryo fibroblast cells (C3H10T1/2).

* Correspondence should be addressed to this author. Telephone: (914) 789-7298; E-mail: dhimant99@hotmail.com.
† American Health Foundation.
‡ U. S. Environmental Protection Agency.

[1] Abbreviations: PAHs, polycyclic aromatic hydrocarbons; DB[*a,l*]P, dibenzo[*a,l*]pyrene; N[1,2-*a*]P, dibenzo[*c,mno*]chrysene (naphtho[1,2-*a*]pyrene); NP, naphthopyrene; N[1,2-*a*]P-9,10-dihydrodiol, (±)-*trans*-9,10-dihydroxy-9,10-dihydro-N[1,2-*a*]P; B[*a*]P-7,8-dihydrodiol, (±)-*trans*-7,8-dihydroxy-7,8-dihydrobenzo[*a*]pyrene; N[1,2-*a*]PDE, (±)-*anti*-9,10-dihydroxy-9,10-dihydro-11,12-epoxy-9,10,11,12-tetrahydro-N[1,2-*a*]P; N[1,2-*e*]P, naphtho[1,2-*e*]pyrene; B[*a*]P, benzo[*a*]pyrene; B[*c*]PhDE, benzo[*c*]phenanthrene diol epoxide; DMBA, 7,12-dimethylbenz[*a*]anthracene.

10.1021/tx0200111 CCC: $22.00
Published on Web 06/20/2002

The formation of PAH-DNA adducts is known to be influenced by the molecular structure of the PAHs. For example, B[*a*]P diol epoxide, a planar molecule, reacts with calf-thymus DNA in vitro to yield exclusively the B[*a*]P-dG adduct (*10*, *11*). However, benzo[*c*]phenanthrene diol epoxide (B[*c*]PhDE), a nonplanar molecule, reacts with calf-thymus DNA to give a mixture of B[*c*]-Ph-dG and B[*c*]Ph-dA adducts (*9*). The relative ratios of dA/dG adducts formed differ depending on the B[*c*]Ph diol epoxide isomers used, but the dA/dG ratios are between 1.4 and 2.0 in favor of the B[*c*]Ph-dA adducts (*9*). This is highly significant because many sterically crowded bay-region PAH-diol-epoxides that favor the formation of PAH-dA adducts are generally more potent carcinogens than their less crowded counterparts. To further verify this steric effect, we examined the pattern of adduct formation between calf-thymus DNA and N[1,2-*a*]PDE in vitro.

Materials and Methods

Synthesis. Melting points were recorded on a Fisher-Johnson melting point apparatus and are uncorrected. Unless stated otherwise, proton NMR spectra were recorded in a Bruker AM 360WB instrument using $CDCl_3$ as solvent. The chemical shifts are reported in ppm downfield from TMS. MS analyses were carried out with a Hewlett-Packard model 5988A instrument. High-resolution MS analyses were determined on a Finnigan Mat95 instrument, at the University of Minnesota. Thin-layer chromatography (TLC) was developed on aluminum-supported, precoated silica gel plates (EM Industries, Gibbstown, NJ). All starting materials were obtained from Aldrich Chemical Co. (Milwaukee, WI) unless stated otherwise. 1-Pyreneboronic acid (**1**) was prepared in quantitative yield by treating 1-bromopyrene with triisopropylborate in the presence of *n*-butyllithium as reported in the literature (*12*). Benzo[*c*]chrysene-5-carboxyaldehyde (**12**) was prepared as reported earlier (*13*).

1-(2-Formylphenyl)pyrene (2). A mixture of 1-pyreneboronic acid (**1**) (1.08 g, 4.4 mmol), 2-bromobenzaldehyde (0.74 g, 4.0 mmol), cesium fluoride (1.34 g, 8.8 mmol), and $Pd(PPh_3)_4$ (0.18 g, 0.16 mmol) in anhydrous DME (30 mL) was heated under reflux for 20 h. The mixture was brought to room temperature, and the reaction was quenched with ice-cold H_2O. The aqueous layer was extracted with CH_2Cl_2 (3 × 25 mL), and the combined organic layers were washed with H_2O, dried ($MgSO_4$), and evaporated to give a crude mixture. This mixture was purified by silica gel column chromatography with hexane/ethyl acetate (99:1) as an eluent to give **2** (0.90 g, 73%) as a pale yellow crystalline solid, mp 118−119 °C: ^{1}H NMR δ 7.59 (d, 1H, J = 7.54 Hz), 7.63−7.81 (m, 1H), 7.75−7.80 (m, 2H), 7.95 (d, 1H, J = 7.87 Hz), 8.02−8.07 (m, 2H), 8.15 (s, 2H), 8.18−8.20 (m, 2H), 8.24−8.27 (m, 2H), 9.66 (s, 1H, CHO); MS m/z 306 (M^+).

1-(2-Formyl-4-methoxyphenyl)pyrene (3). In a similar manner, reacting 1-pyreneboronic acid (**1**) (3.60 g, 14.6 mmol), 2-bromo-5-methoxybenzaldehyde (2.86 g, 13.3 mmol), CsF (4.44 g, 29.3 mmol), and $Pd(PPh_3)_4$ (0.61 g, 0.53 mmol) in anhydrous DME (100 mL) gave crude **3** which was purified on a silica gel column with hexane/ethyl acetate (98:2) as an eluent to yield 4.1 g (92%) of aldehyde **3** as a pale yellow crystalline solid, mp 201−202 °C: ^{1}H NMR δ 3.99 (s, 3H, OCH_3), 7.33 (dd, 1H, H5′, $J_{5',3'}$ = 2.9 Hz and $J_{5',6'}$ = 8.2 Hz), 7.50 (d, 1H, H6′, $J_{6',5'}$ = 8.2 Hz), 7.67 (d, 1H, H3′, $J_{3',5'}$ = 2.9 Hz), 7.79 (d, 1H, H9, $J_{9,10}$ = 9.2 Hz), 7.93 (d, 1H, H3, $J_{2,3}$ = 7.5 Hz), 8.01−8.06 (m, 2H, H7 and H10), 8.14 (s, 2H, H4 and H5), 8.19 (d, 1H, H8, $J_{7,8}$ = 7.87), 8.24 (d, 2H, H2 and H6, $J_{2,3}$ = 7.5 Hz), 9.61 (s, 1H, CHO); high-resolution MS m/z calcd for $C_{24}H_{16}O_2$, 336.1153; found, 336.1150.

1-[2-(β-Methoxyethenyl)phenyl]pyrene (4). A suspension of anhydrous (methoxymethyl)triphenylphosphonium chloride (3.3 g, 9.6 mmol) in freshly distilled diethyl ether (dried over sodium, 60 mL) was cooled to −78 °C under N_2. To this mixture was added PhLi (1.8 M, 4.0 mL, 7.2 mmol) in cyclohexane/ether (70:30), dropwise, and the mixture was stirred for 30 min. The reaction mixture was then allowed to warm to −30 °C, stirred for another 30 min, and again cooled to −78 °C. A solution of **2** (0.6 g, 1.9 mmol) in THF (40 mL) was then added dropwise, and the mixture was allowed to come to room temperature and left overnight. The reaction was quenched with 1 N HCl; the mixture was washed several times with water and extracted with ethyl acetate (3 × 25 mL). The combined organic layers were dried ($MgSO_4$), filtered, and concentrated. The resulting residue was purified on a silica gel column by elution with hexane/ethyl acetate (98:2) to yield a mixture of cis- and trans-isomers of olefin **4** (0.52 g, 81%), as a clear viscous oil: ^{1}H NMR δ 3.21 (s, 1.55H, *trans*-OCH_3), 3.72 (s, 1.45H, *cis*-OCH_3), 4.81 (d, 0.48H, *cis*-olefin H, J = 7.2 Hz), 5.43 (d, 0.52H, *trans*-olefin H, J = 12.8 Hz), 5.85 (d, 0.48H, *cis*-olefin H, J = 7.2 Hz), 7.00 (d, 0.52H, *trans*-olefin H, J = 12.8 Hz,), 7.34−7.55 (m, 3H), 7.61 (d, 0.5H, cis/trans, J = 7.5 Hz), 7.80−7.84 (m, 1H), 7.93−7.95 (m, 1H), 7.98−8.05 (m, 2H), 8.13−8.25 (m, 5H), 8.35 (d, 0.5H, cis/trans, J = 7.8 Hz); MS m/z 334 (M^+).

1-[2-(β-Methoxyethenyl)-4-methoxyphenyl]pyrene (5). Olefin **5** was prepared by following a procedure similar to that used for compound **4**, namely, reacting anhydrous (methoxymethyl)triphenylphosphonium chloride (21.4 g, 62.5 mmol) in freshly distilled Et_2O (400 mL) with PhLi (1.8 M, 26 mL, 46.9 mmol) in cyclohexane/ether (70:30), and **3** (4.2 g, 12.5 mmol) in THF (300 mL). The resulting crude olefin **5** was purified on a silica gel column. Elution with hexane/ethyl acetate (97:3) yielded a mixture of cis- and trans-isomers of olefin **5** (3.83 g, 84%): ^{1}H NMR δ 3.19 (s, 1.65H, *trans*-OCH_3), 3.72 (s, 1.35H, *cis*-OCH_3), 3.94 (s, 1.35H, *cis*-OCH_3), 3.95 (s, 1.65H, *trans*-OCH_3), 4.76 (d, 0.45H, *cis*-olefin H, J = 7.2 Hz), 5.38 (d, 0.55H, *trans*-olefin H, J = 13.1 Hz), 5.85 (d, 0.45H, *cis*-olefin H, J = 7.2 Hz), 6.89−6.93 (m, 1H), 6.98 (d, 0.55H, *trans*-olefin H, J = 12.8 Hz), 7.11 (d, 0.55H, *trans*-H3′, J = 2.6 Hz), 7.28−7.32 (m, 1H, H6′), 7.79−7.83 (m, 1H), 7.89 (d, 0.45H, *cis*-H3′, J = 2.0 Hz), 7.90−7.93 (m, 1H), 7.96−8.04 (m, 2H), 8.91−8.23 (m, 5H); MS m/z 364 (M^+).

Naphtho[1,2-*a*]pyrene (N[1,2-*a*]P) (6). To a solution of olefin **4** (0.4 g, 1.2 mmol) in anhydrous CH_2Cl_2 (30 mL) was added CH_3SO_3H (5 mL) dropwise under N_2, and the mixture was stirred at room temperature for 2 h. It was then poured into ice-cold H_2O, and the organic layer was separated, and washed successively with 10% $NaHCO_3$ solution and several times with water. The organic layer was dried ($MgSO_4$) and evaporated, and the crude residue was purified on a silica gel column with hexane/ethyl acetate (99:1) to give **6** (0.33 g, 91%), as a pale yellow crystalline solid; mp 166−167 °C, lit (*14*, *15*) mp 216−218 °C: ^{1}H NMR δ 7.68−7.81 (m, 2H, H10 and H11), 7.96 (d, 1H, J = 8.9 Hz), 8.02−8.22 (m, 6H), 8.29 (d, 1H, J = 7.9 Hz), 8.34 (d, 1H, H14, $J_{13,14}$ = 9.2 Hz), 8.57 (s, 1H, H6), 9.27 (d, 1H, H12, $J_{11,12}$ = 8.5 Hz), 9.44 (d, 1H, H13, $J_{13,14}$ = 9.2 Hz); high-resolution MS m/z calcd for $C_{24}H_{14}$, 302.1096; found, 302.1093.

10-Methoxy-N[1,2-*a*]P (7). By following a procedure identical to that used above, the methoxy derivative **7** was prepared by reacting olefin **5** (3.64 g, 10 mmol) in anhydrous CH_2Cl_2 (50 mL) and CH_3SO_3H (25 mL). The crude residue was purified on a silica gel column with hexane/ethyl acetate (97:3) to give **7** (2.3 g, 77%) as a pale yellow crystalline solid, mp 192−193 °C: ^{1}H NMR δ 4.05 (s, 3H, OCH_3), 7.39 (dd, 1H, H11, $J_{9,11}$ = 2.6 Hz, $J_{11,12}$ = 9.2 Hz), 7.46 (d, 1H, H9, $J_{9,11}$ = 2.6 Hz), 7.88 (d, 1H, J = 8.9 Hz), 8.01−8.18 (m, 5H), 8.26 (d, 1H, J = 7.9 Hz), 8.29 (d, 1H, H14, $J_{14,13}$ = 9.2 Hz), 8.53 (s, 1H, H6), 9.16 (d, 1H, H12, $J_{12,11}$ = 9.2 Hz), 9.34 (d, 1H, H13, $J_{13,14}$ = 9.2 Hz); high-resolution MS m/z calcd for $C_{25}H_{16}O$, 332.1199; found, 332.1193.

10-Hydroxy-N[1,2-*a*]P (8). To a stirred solution of 10-methoxy-N[1,2-*a*]P (**7**) (2.09 g, 6.03 mmol) in CH_2Cl_2 (180 mL) at room temperature was added dropwise a solution of BBr_3 (1 M solution in CH_2Cl_2, 12.6 mL, 12.6 mmol) under N_2 over 10 min. After continuous stirring at room temperature for 5 h, the

reaction was quenched with ice-cold H_2O. The organic layer was washed several times with water, and dried over $MgSO_4$. Removal of the solvent gave the crude solid that was purified by column chromatography with hexane/ethyl acetate (10:1) to yield **8** (1.36 g, 68%) as a pale yellow crystalline solid, mp 216−218 °C: ^{1}H NMR δ 5.13 (s, 1H, OH), 7.32 (dd, 1H, H11, $J_{9,11}$ = 2.9 Hz, $J_{11,12}$ = 9.2 Hz), 7.45 (d, 1H, H9, $J_{9,10}$ = 2.9 Hz), 7.83 (d, 1H, J = 8.9 Hz), 8.02−8.08 (m, 3H), 8.13 (d, 1H, J = 8.9 Hz), 8.18 (d, 1H, J = 7.5 Hz), 8.27 (d, 1H, J = 6.9 Hz), 8.30 (d, 1H, H14, $J_{13,14}$ = 9.2 Hz), 8.54 (s, 1H, H6), 9.15 (d, 1H, H12, $J_{12,11}$ = 9.2 Hz), 9.33 (d, 1H, H13, $J_{13,14}$ = 9.2 Hz); high-resolution MS *m*/*z* calcd for $C_{24}H_{14}O$, 318.1045; found, 318.1045.

N[1,2-*a*]P-9,10-dione (9). To a stirred suspension of the hydroxy derivative, **8** (1.24 g, 3.9 mmol) in a mixture of CH_2Cl_2/C_6H_6/THF (60:180:6) (246 mL) and Adogen 464 (3 drops), was added an aqueous solution of KH_2PO_4 (0.17 M, 210 mL) and Fremy's salt (3.14 g, 11.7 mmol). The reaction mixture was stirred at room temperature for 3 h and then diluted with CH_2Cl_2. The organic layer was separated, washed with water (3 × 50 mL), dried ($MgSO_4$), and filtered. The crude residue obtained after removal of the solvent was washed several times with a mixture of hexane/acetone (8:2) to give **9** (0.97 g, 75%) as a dark red solid, mp 190−191 °C: ^{1}H NMR δ 6.51 (d, 1H, H11, $J_{11,12}$ = 10.5 Hz), 7.95 (d, 1H, J = 8.9 Hz), 8.00 (d, 1H, J = 6.9 Hz), 8.06 (t, 1H, H2, J = 7.8 Hz), 8.17 (d, 1H, J = 6.9 Hz), 8.20 (d, 1H, J = 8.5 Hz), 8.28−8.33 (m, 4H), 8.53 (d, 1H, H12, $J_{11,12}$ = 10.5 Hz), 8.56 (d, 1H, H13, $J_{13,14}$ = 8.9 Hz); high-resolution MS *m*/*z* calcd for $C_{24}H_{12}O_2$, 332.0838; found, 332.0837.

(±)-*trans*-9,10-Dihydroxy-9,10-dihydro-N[1,2-*a*]P (10). To a suspension of dione **9** (0.15 g, 0.45 mmol) in ethanol (300 mL) was added $NaBH_4$ (0.51 g, 13.5 mmol) in several portions over 10 min. The mixture was stirred for 48 h at room temperature while a stream of oxygen was bubbled through the solution. The solution was then concentrated under reduced pressure to one-fourth of its original volume. This concentrate was diluted with H_2O, and extracted with EtOAc (3 × 30 mL). The organic layer was dried (Na_2SO_4), filtered, and concentrated, and the resulting residue was washed with a mixture of hexane/diethyl ether (9:1) to give diol **10**. Purification by column chromatography using methylene chloride with gradually increasing ethyl acetate gave diol **10** (0.12 g, 79%), mp 225−227 °C: ^{1}H NMR (DMSO-d_6) δ 4.59−4.65 (m, 1H, H10), 4.69 (dd, 1H, H9, $J_{9,10}$ = 11.5 Hz, $J_{OH,9}$ = 5.9 Hz), 5.42 (d, 1H, OH, $J_{OH,10}$ = 4.9 Hz), 5.77 (d, 1H, OH, $J_{OH,9}$ = 5.9 Hz), 6.36 (dd, 1H, H11, $J_{11,12}$ = 10.1 Hz, $J_{10,11}$ = 1.5 Hz), 7.39 (d, 1H, H12, $J_{11,12}$ = 10.1 Hz), 8.01−8.10 (m, 4H), 8.21 (d, 1H, J = 7.2 Hz), 8.28−8.38 (m, 3H), 8.64 (s, 1H, H6), 8.95 (d, 1H, H13, $J_{13,14}$ = 9.19 Hz); high-resolution MS *m*/*z* calcd for $C_{24}H_{16}O_2$, 336.1150; found, 336.1150.

(±)-*anti*-9,10-Dihydroxy-9,10-dihydro-11,12-epoxy-9,10,-11,12-tetrahydro-N[1,2-*a*]P (11). A solution of dihydrodiol **10** (0.10 g, 0.3 mmol) and *m*CPBA (0.52 g, 3.0 mmol) in freshly distilled THF (100 mL) was stirred at room temperature under N_2 and monitored by normal-phase HPLC using an analytical Licrosorb Si60 column (5 μm) (E. Merck, Darmstadt, Germany) with hexane/THF (75:25) in an isocratic program at a flow rate of 1.9 mL/min. After 7 h of stirring, the mixture was diluted with 150 mL of diethyl ether, washed with cold 2% NaOH (2 × 100 mL) and water (3 × 150 mL), and then dried (K_2CO_3), filtered, and concentrated at room temperature. The concentrate was washed with a mixture of hexane/diethyl ether (75:25, 50 mL) and dried in vacuo to yield diol epoxide **11** (0.08 g, 76%) as a pale, yellow solid, mp 191−193 °C: ^{1}H NMR (DMSO-d_6) δ 3.80 (d, 1H, H11, $J_{11,12}$ = 4.3 Hz), 3.87 (d, 1H, H10, $J_{9,10}$ = 8.3 Hz), 4.76 (d, 1H, H9, $J_{9,10}$ = 8.3 Hz), 4.98 (d, 1H, H12, $J_{11,12}$ = 4.3 Hz), 8.01−8.14 (m, 4H), 8.23 (d, 1H, J = 7.2 Hz), 8.36 (d, 1H, J = 8.9 Hz), 8.39 (d, 1H, J = 8.9 Hz), 8.43 (d, 1H, H14, $J_{14,13}$ = 9.2 Hz), 8.68 (s, 1H, H6), 9.06 (d, 1H, H13, $J_{13,14}$ = 9.2 Hz); high-resolution MS *m*/*z* calcd for $C_{24}H_{16}O_3$, 352.1097; found 352.1099.

5-(*β*-Methoxyethenyl)benzo[*c*]chrysene (13). By following a procedure similar to that used for compound **4**, benzo[*c*]-chrysene derivative **13** was prepared by using (methoxymethyl)-triphenylphosphonium chloride (21.4 g, 62.5 mmol), PhLi (1.8 M, 26 mL, 46.9 mmol), and aldehyde **12** (3.8 g, 12.5 mmol). The crude product **13** was purified on a silica gel column by elution with hexane/ethyl acetate (97:3) to yield a mixture of the major *trans*-isomer and a minor *cis*-isomer of olefin **13** (3.43 g, 82%): ^{1}H NMR δ 3.88 (s, 2.85H, *trans*-OCH_3), 3.90 (s, 0.15H, *cis*-OCH_3), 6.10 (d, 0.05H, *cis*-olefin H, J = 7.2 Hz), 6.50 (d, 0.05H, *cis*-olefin H, J = 7.2 Hz), 6.71 (d, 0.95H, *trans*-olefin H, J = 12.5 Hz), 7.21 (d, 0.95H, *trans*-olefin, J = 12.5 Hz), 7.58−7.69 (m, 4H, H2, H3, H10, and H11), 7.82−7.91 (m, 4H, H6, H7, H8, and H14), 7.91−8.03 (m, 2H, H1 and H9), 8.90 (d, 1H, H12, $J_{12,11}$ = 7.5 Hz), 8.91 (d, 1H, H13, $J_{13,14}$ = 9.2 Hz), 9.19 (d, 1H, H4, $J_{3,4}$ = 7.9 Hz); MS *m*/*z* (relative intensity) 334 (M^+, 60), 303 (M^+−OCH3, 100), 289 (50).

Naphtho[1,2-*a*]pyrene (N[1,2-*a*]P) (6). In a nitrogen atmosphere, to a solution of olefin **13** (3.34 g, 10 mmol) in anhydrous CH_2Cl_2 (50 mL) was added dropwise CH_3SO_3H (25 mL), and the mixture was stirred at room temperature for 3 h. It was then poured into ice-cold H_2O, and the organic layer was separated and washed successively with 10% $NaHCO_3$ solution and several times with water. The organic layer was dried ($MgSO_4$) and evaporated, and the crude residue was purified on a silica gel column with hexane/ethyl acetate (97:3) as an eluent to give **6** (2.1 g, 69%) as a pale yellow crystalline solid, mp 166−167 °C.

In Vitro Metabolism of Naphtho[1,2-a]pyrene with Phenobarbital/*β*-Naphthoflavone-Induced Male Sprague Dawley Rat S9 Liver Homogenate. N[1,2-*a*]P (2 mg in 200 μL of DMSO) was incubated at 37 °C for 20 min, in the presence of cofactors and 8 mL of the 9000*g* supernatant from livers of phenobarbital/*β*-naphthoflavone-induced male Sprague Dawley rats (*16*). The mixture was extracted with EtOAc (3 × 30 mL), dried ($MgSO_4$), filtered, and concentrated at reduced pressure to give a residue that was dissolved in methanol. The metabolites of N[1,2-*a*]P were analyzed by HPLC on a 4.6 × 250 mm (5 μm) Vydac C18 reverse-phase column (Separation Group, Hesperia, CA) with solvent A (H_2O) and solvent B (methanol), using a gradient program from A:B (50:50) to A:B (0:100) over 40 min.

Mutagenicity Assays. N[1,2-*a*]P, N[1,2-*a*]P-9,10-dihydrodiol, B[*a*]P, and B[*a*]P-7,8-dihydrodiol were each dissolved in DMSO and assayed in *S. typhimurium* strain TA 100 with 20 min of preincubation according to an established method (*17*). In these studies, 50 μL of phenobarbital/*β*-naphthoflavone-induced male Sprague Dawley rat liver homogenate *S*9 mix (75 mg of protein/mL) was used per plate, and sodium azide at a dose of 5 μg/plate (1008 His-rev/plate) was the positive control. Values are reported as the mean ± SD (n = 3). Background counts for solvent (121 His-rev/plate) have not been subtracted.

Morphological Cell Transformation: Cell Culture. Cells from the mouse embryo fibroblast cell line C3H10T1/2Cl8 (passage 8), derived by Reznikoff et al., were utilized in this study (*18*). Cells were incubated at 85% relative humidity in an atmosphere containing 5% CO_2 in air at 37 °C. The cultures were grown in Eagle's basal medium with Earle's salts and L-glutamine, supplemented with 10% heat-inactivated fetal bovine serum (Grand Island Biological Co., Grand Island, NY). The cells were checked on a routine basis for mycoplasma contamination by the Gibco MycoTect assay and were found to be mycoplasma-free.

Morphological Cell Transformation Assays. The morphological cell transformation and cytotoxicity procedures of Mohapatra et al. (*19*) for C3H10T1/2 cells were used without modification. C3H10T1/2 cells were seeded for cytotoxicity studies (6 dishes per concentration) at 200 cells per 60-mm plastic Petri dish and for transformation studies (24 dishes per concentration) at 1000 cells per 60-mm plastic Petri dish in 5 mL of medium. The cells were treated with N[1,2-*a*]P or B[*a*]P dissolved in acetone (25 μL) 24 h after seeding. After a 24-h exposure, the cells were fed with fresh complete medium containing 25 μg/mL Garamycin. Seven to ten days after the treatment, the cytotoxicity dishes were fixed with methanol and

Scheme 1. Syntheses of Naphtho[1,2-*a*]pyrene, *trans*-Naphtho[1,2-*a*]pyrene-9,10-dihydro Diol, and *anti*-Naphtho[1,2-*a*]pyrene-9,10-dihydrodiol-11,12-epoxide

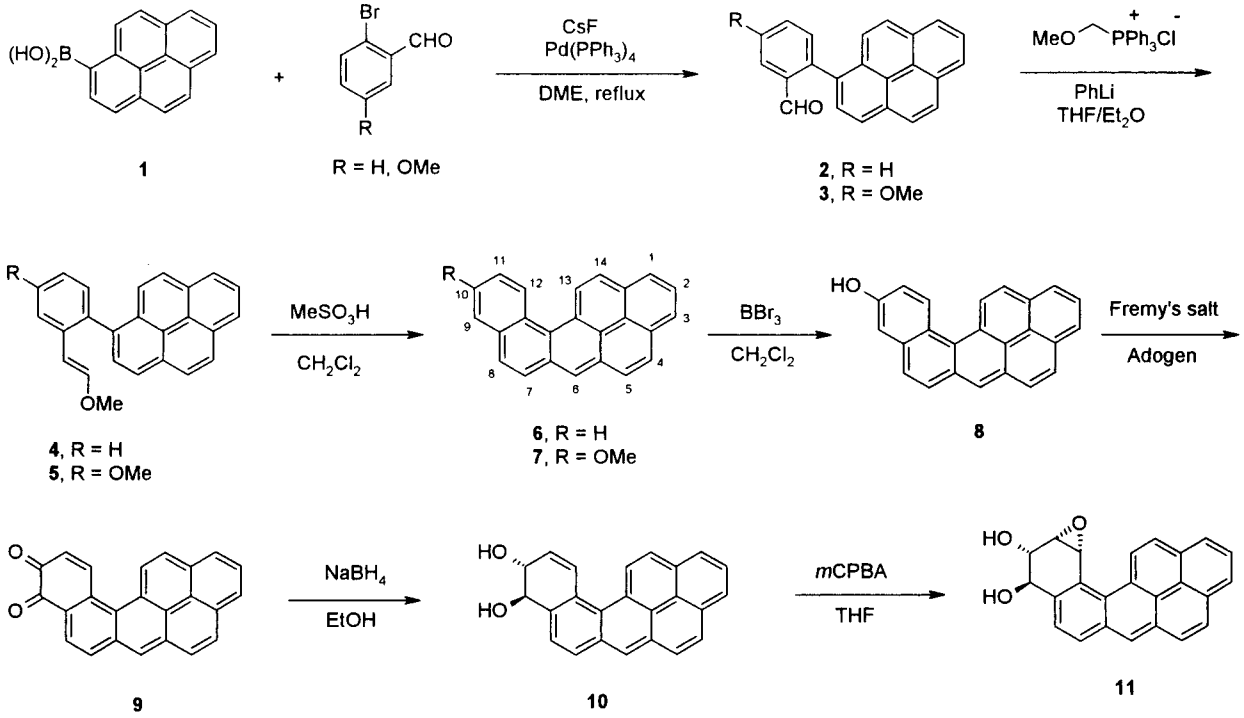

1 R = H, OMe

2, R = H
3, R = OMe

4, R = H
5, R = OMe

6, R = H
7, R = OMe

8

9

10

11

stained with Giemsa. The colonies were then counted. The medium in the cell transformation dishes was changed weekly. At confluence, the fetal bovine serum level was reduced to 5%. At the end of 6 weeks, the dishes were fixed, stained with Giemsa, and scored for morphological transformation according to published criteria (*20*).

Preparation of DNA Adducts. *anti*-N[1,2-*a*]PDE (**11**) (1 mg) in 1.0 mL of THF was added to a solution of calf thymus DNA (10 mg) in 10 mL of 10 mM Tris-HCl buffer, pH 7. This mixture was incubated at 37 °C. The DNA was isolated and enzymatically hydrolyzed to deoxyribonucleosides as described in the literature (*21*). Modified deoxyribonucleosides were analyzed by HPLC as described below.

Preparation of the Standard 2′-dGuo or 2′-dAdo Adducts from Diol Epoxide. Approximately 100 mg each of 2′-dGuo-5′-monophosphate or 2′-dAdo-5′-monophosphate was dissolved in 10 mL of 10 mM Tris-HCl buffer (pH 7.0). Then *anti*-N[1,2-*a*]PDE (**11**) (1 mg) in 1.0 mL of acetone/THF (50:50) was added, and the solution was incubated overnight at 37 °C. The modified deoxyribonucleotides were separated from unmodified deoxyribonucleotides on Sep-Pak C_{18} cartridges. They were then enzymatically hydrolyzed to the corresponding deoxyribonucleosides (*21*), and analyzed by HPLC with a Beckman Ultrasphere ODS 5-μm column (4.6 × 250 mm; reverse phase) using the following solvent system: 46% MeOH in H_2O for 10 min, followed by a linear gradient from 46 to 60% MeOH in H_2O over 40 min, then 90% MeOH in H_2O for 10 min at a flow rate of 1 mL/min.

Results and Discussion

This report describes a new convenient synthesis of N[1,2-*a*]P that uses the Suzuki coupling reaction as shown in Scheme 1. The Suzuki coupling reaction was recently introduced for the syntheses of PAH ring systems because it can readily be adapted to a large scale and gives high yields (*22*−*25*). The palladium-catalyzed reaction of 1-pyreneboronic acid (**1**) and 2-bromobenzaldehyde gave compound **2** in 73% yield. Treatment of aldehyde **2** with (methoxymethyl)triphenylphosphonium

Scheme 2. Synthesis of Naphtho[1,2-*a*]pyrene

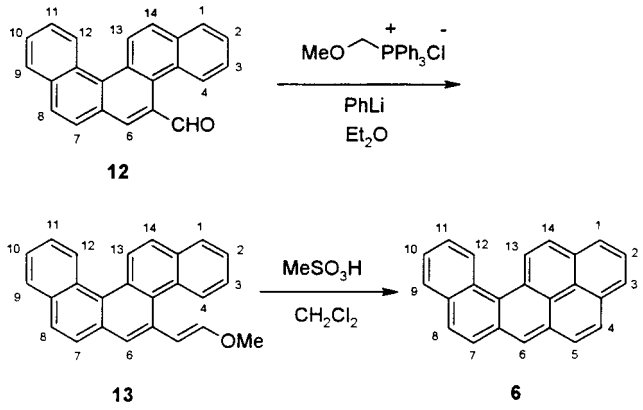

12

13

6

chloride resulted in the formation of olefin **4** which cyclized readily in the presence of $MeSO_3H$ to give N[1,2-*a*]P (**6**) in 77% yield. Interestingly, the melting point of N[1,2-*a*]P thus obtained (166−167 °C) differed from that reported earlier (216−218 °C) (*14*,*15*). This implied that the product reported earlier (*15*) was perhaps not N[1,2-*a*]P.

To confirm the structure, we thought it worthwhile to develop an alternate route for the synthesis of N[1,2-*a*]P (Scheme 2). Compound **12** on treatment with (methoxymethyl)triphenylphosphonium chloride afforded the olefin **13** which, on acid-catalyzed cyclization with methanesulfonic acid, gave N[1,2-*a*]P (**6**) in quantitative yield. The N[1,2-*a*]P thus obtained showed MS, NMR, UV, and mp identical to those obtained earlier by the Suzuki coupling reaction and, thus, confirmed the assigned structure **6**. These data were also identical to those reported recently by S. Kumar (*22*).

We also describe here the syntheses of the putative proximate carcinogenic metabolite N[1,2-*a*]P-9,10-dihydrodiol (**10**) and the ultimate carcinogenic metabolite

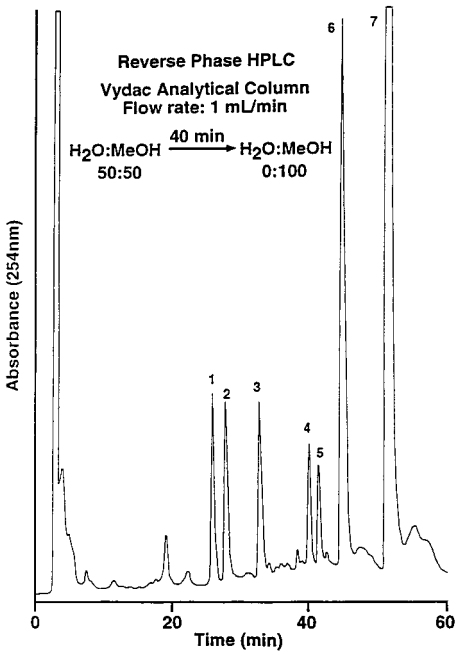

Figure 1. HPLC profile of in vitro metabolites of N[1,2-*a*]P.

Table 1. Metabolism of N[1,2-*a*]P with Phenobarbital/ *β*-Naphthoflavone-Induced Male Sprague Dawley Rat Liver Homogenate[a]

peak number	metabolite identified
1	4,5-dihydroxy-4,5-dihydro-N[1,2-*a*]P
2	7,8-dihydroxy-7,8-dihydro-N[1,2-*a*]P
3	9,10-dihydroxy-9,10-dihydro-N[1,2-*a*]P
4	1- or 3-hydroxy-N[1,2-*a*]P
5	10-hydroxy-N[1,2-*a*]P
6	1- or 3-hydroxy-N[1,2-*a*]P
7	N[1,2-*a*]P

[a] For experimental conditions, see text.

N[1,2-*a*]PDE (**11**). The key intermediate 10-methoxy-N[1,2-*a*]P (**7**) was obtained by applying the Suzuki coupling reaction as depicted in Scheme 1. Demethylation of **7** with BBr_3 afforded 10-hydroxy-N[1,2-*a*]P (**8**) which, on oxidation with Fremy's salt, gave quinone **9**. The reduction of **9** with $NaBH_4$ in EtOH furnished N[1,2-*a*]P-9,10-dihydrodiol (**10**) in 79% yield. Dihydrodiol **10**, on further oxidation with *m*CPBA, yielded N[1,2-*a*]PDE (**11**). The structures of dihydrodiol **10** and diol epoxide **11** were assigned on the basis of their ^{1}H NMR and mass spectra. The trans structure was assigned to dihydrodiol **10** on the basis of the observed coupling constant of 10.5 Hz between protons H9 and H10 in its ^{1}H NMR spectrum.

The in vitro metabolism study of N[1,2-*a*]P was carried out with male Sprague Dawley rat liver *S*9 fraction pretreated with phenobarbital/*β*-naphthoflavone. The HPLC profile of metabolites is shown in Figure 1, and the assignments for the metabolites are listed in Table 1. Each metabolite was collected from the HPLC and characterized by UV, MS, ^{1}H and NMR spectroscopic methods. Assignments of ^{1}H NMR spectra of metabolites 1−3 are shown in Figure 2. Metabolites were further confirmed by HPLC co-injection of the synthetic standards. Metabolites 1 and 2 were identified as 4,5-dihydroxy-4,5-dihydro-N[1,2-*a*]P and 7,8-dihydroxy-7,8-dihydro-N[1,2-*a*]P, respectively. The spectral properties of metabolite 3 were identical to those obtained from the synthetic *trans*-N[1,2-*a*]P-9,10-dihydrodiol (**10**); therefore,

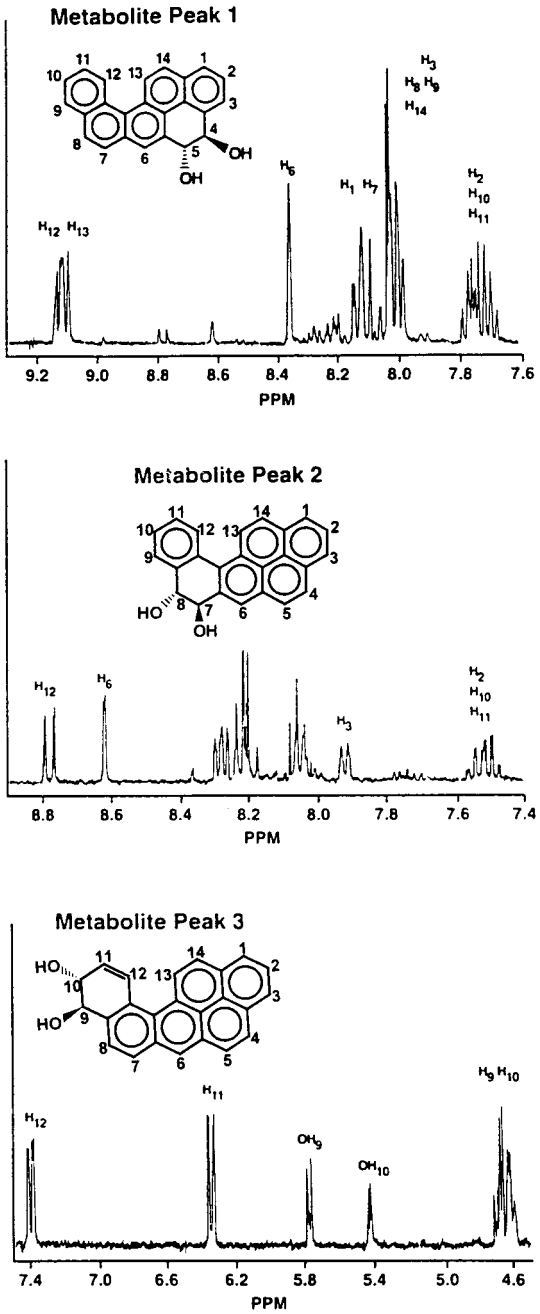

Figure 2. Proton NMR spectra of N[1,2-*a*]P metabolites 1−3.

it was assigned as *trans*-N[1,2-*a*]P-9,10-dihydrodiol (**10**). In a similar fashion, metabolite 5 was identified as 10-hydroxy-N[1,2-*a*]P (**8**), while metabolites 4 and 6 were identified as 1-hydroxy- and/or 3-hydroxy-N[1,2-*a*]P based on our analysis of ^{1}H NMR and mass spectra.

The bacterial mutagenicity assay with *S. typhimurium* TA100 is shown in Figure 3A and 3B. B[*a*]P and B[*a*]P-7,8-dihydrodiol were used as positive controls (*26*). N[1,2-*a*]P-9,10-dihydrodiol appears to be a proximate mutagen since it was more mutagenic than N[1,2-*a*]P. B[*a*]P and N[1,2-*a*]P showed similar mutagenic activity up to 4 nmol/plate and above 4 nmol/plate, N[1,2-*a*]P was more toxic. The corresponding dihydrodiols, namely, B[*a*]P-7,8-dihydrodiol and N[1,2-*a*]P-9,10-dihydrodiol showed similar mutagenic activity up to 2 nmol/plate; however, at 4 nmol/plate, N[1,2-*a*]P-9,10-dihydrodiol was half as mutagenic as B[*a*]P-7,8-dihydrodiol. Dihydrodiol metabolites were more mutagenic than their corresponding hydro-

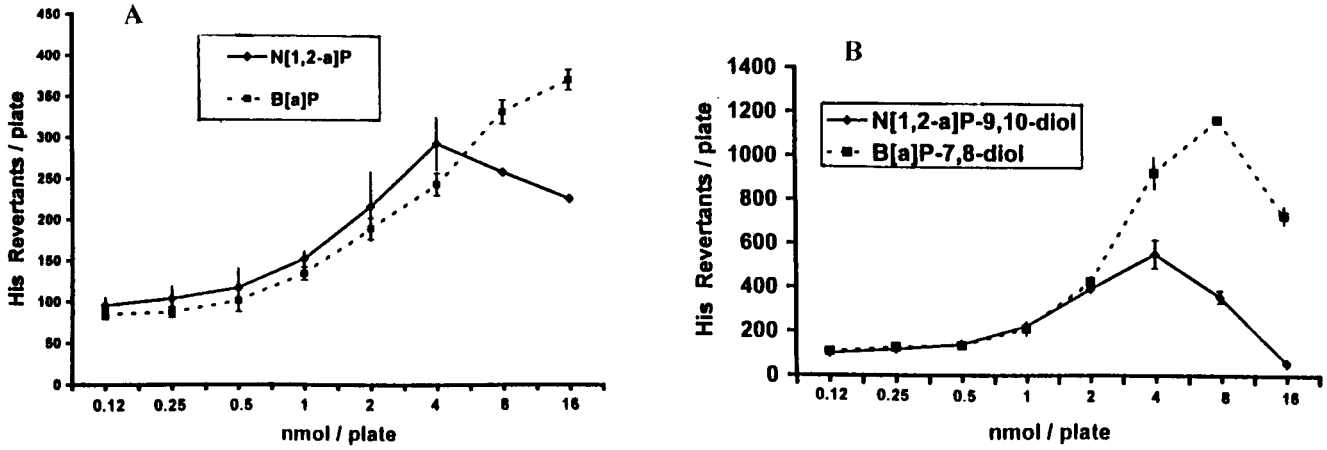

Figure 3. (A) Mutagenicity assay of B[*a*]P and N[1,2-*a*]P toward *S. typhimurium* strain TA 100. (B) Mutagenicity assay with B[*a*]P-7,8-dihydrodiol and N[1,2-*a*]P-9,10-dihydrodiol toward *S. typhimurium* strain TA 100.

Table 2. Cytotoxicity and Morphological Cell Transformation of C3H10T1/2 Cells by N[1,2-a]P and B[*a*]P

compound	concn (μM)	% survival, mean ± SD[a]	total no. of Type II foci[b]	total no. of Type III foci[b]	Types II&III foci/dish, mean ± SD[b]	% dishes with Type II or III foci, mean ± SD[b]
acetone	0.5%	100 ± 0	2	0	0.03 ± 0.04	2.9 ± 4.1
N[1,2-*a*]P	0.03	95.3 ± 7.5	0	2	0.03 ± 0.04	2.8 ± 3.9
	0.09	84 ± 6.5[c]	4	0	0.07 ± 0.07	7.2 ± 6.9
	0.19	73.8 ± 6.5[c]	4	6	0.14 ± 0.11	12.8 ± 9.2
	0.31	68.5 ± 5.7[c]	16	9	0.35 ± 0.20[d]	32.1 ± 19.2[d]
	0.99	65.1 ± 5.5[c]	34	24	0.83 ± 0.43[c]	54.4 ± 14.5[c]
	1.99	59.5 ± 8.4[c]	43	19	0.86 ± 0.22[c]	59.7 ± 10.9[c]
	3.31	51.7 ± 10.7[c]	37	13	0.69 ± 0.31[c]	50.0 ± 18.9[c]
B[*a*]P	0.39	95.5 ± 0.8	1	1	0.05 ± 0.05[e]	4.4 ± 4.4[e]
	1.2	81.3 ± 7.0[c]	14	16	0.74 ± 0.07[c,e]	50.2 ± 4.7[c,e]
	3.97	74.6 ± 3.3[c]	24	30	0.94 ± 0.28[c]	56.5 ± 14.2[c]

[a] The mean plating efficiency in untreated C3H10T1/2 cells was 29.9%. The survival data are based on 3 replicate studies; each study consisted of 6 dishes per group plated and scored. [b] Based on 3 replicate studies; each study consisted of 24 dishes per group plated and scored. [c] Statistically different from the corresponding acetone control group at $p < 0.05$ by the multiple comparison, Bonferroni *t*-test. [d] One of the 3 replicate studies was significantly different ($p < 0.05$) from the acetone control while the remaining 2 showed marginal results. [e] Results from two replicate studies.

carbons in TA 100 system. Above 4 nmol/plate N[1,2-*a*]P-9,10-dihydrodiol was also more toxic than B[*a*]P-7,8-dihydrodiol.

Both N[1,2-*a*]P and B[*a*]P were cytotoxic to C3H10T1/2 cells as measured by reductions in plating efficiency (Table 2). In triplicate studies over a concentration range of 0−3.31 μM, N[1,2-*a*]P produced a smooth survival curve to a maximal effect of 51.7% of control. Statistical significance ($p < 0.05$) was achieved at equal to or greater than 0.09 μM. Over an analogous concentration range, B[*a*]P produced significant but slightly less cytotoxicity. Morphological cell transformation measured as the induction of transformed Type II and Type III foci was determined over the same concentration ranges as the cytotoxicity studies. In triplicate studies, statistically significant increases over control ($p < 0.05$) in the incidences of dishes exhibiting a Type II or III transformed focus were observed at concentrations of 1.99 and 3.31 μM N[1,2-*a*]P. Up to 59.7% of the dishes exhibited a Type II or III focus. B[*a*]P also produced statistically significant numbers of dishes with morphologically altered transformed C3H10T1/2 cells ($p < 0.05$) at 1.2 and 3.97 μM, giving a maximal level of 56.5% of the dishes exhibiting a Type II or III focus. The numbers of Type II and III transformed foci/dish also were highly significant compared to control ($p < 0.05$) at concentrations of 1.99 and 3.31 μM N[1,2-*a*]P and at 1.2 and 3.97 μM B[*a*]P.

The C3H10T1/2 morphological cell transformation studies indicated that N[1,2-*a*]P and B[*a*]P were approximately similar in transformation activity. Comparison of the activity of N[1,2-*a*]P with that of other potent transforming agents in C3H10T1/2 cells including DB-[*a,l*]P, B[*a*]P, 7,12-dimethylbenz[*a*]anthracene (DMBA), dibenz[*a,h*]anthracene, and 3-methylcholanthrene indicated the order of activity of to be: DMBA > DB[*a,l*]P > N[1,2-*a*]P, B[*a*]P > dibenz[*a,h*]anthracene > 3-methylcholanthrene (*27*). DB[*a,l*]P and DMBA were able to transform C3H10T1/2 cells at lower concentrations (*27*). These results predict the strong potential for N[1,2-*a*]P as a tumorigen in vivo because all of the aforementioned PAHs have been shown to be mouse skin and mouse lung tumorigens (*28*).

Fjord region diol epoxides derived from numerous PAHs are known to favor reaction with dA over reaction with dG; therefore, we examined the formation pattern of in vitro adducts with calf-thymus DNA and N[1,2-*a*]-PDE. At first, we prepared nucleoside markers from N[1,2-*a*]PDE (**11**) with either 2′-dG-5′-monophosphate or 2′-dA-5′-monophosphate. The modified deoxyribonucleotides were enzymatically hydrolyzed to deoxyribonucleosides, which were analyzed by HPLC (panels A and B, Figure 4). Then, the N[1,2-*a*]P diol epoxide (**11**) was incubated with calf-thymus DNA, and the modified DNA was isolated and digested enzymatically to give nucleo-

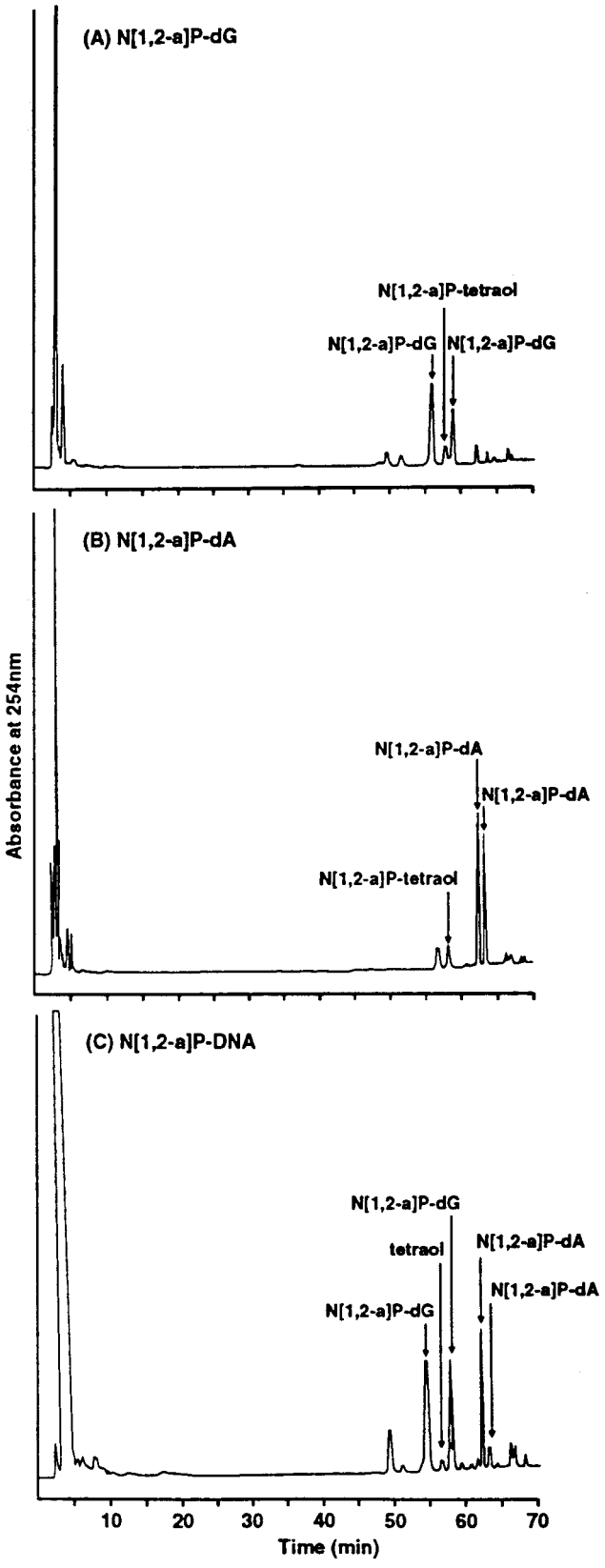

Figure 4. HPLC profile of N[1,2-*a*]P dA, dG, and calf-thymus DNA adducts.

side adducts. Their HPLC analysis is shown in panel C of Figure 4. Peaks 1 and 3 were identified as adducts of dG and peaks 4 and 5 as adducts of dA by comparison of their retention times to those of the standard markers. The total adduct formation for dG is 2.9-fold higher than that of dA-adducts. This is higher than the dG/dA ratio for 3,4-dihydro-1,2-epoxy-1,2,3,4-tetrahydrobenzo[*c*]phenanthrene, which is 0.5−0.7, yet it is lower (*9*) than the dG/dA ratio of 20 for 7,8-dihydroxy-9,10-epoxy-7,8,9,10-tetrahydrobenzo[*a*]pyrene (*10*). Our observation is consistent with the trend that fjord region diol epoxides enhance the levels of dA-adducts. It is also in line with our observation on the adduct formation of 9,10-dihydroxy-11,12-epoxy-9,10,11,12-tetrahydrobenzo[*c*]chrysene which yielded 2.6 times more dG-adducts than dA-adducts (*29*). Collectively, these results suggest that the degree of distortion at the crowded fjord region of benzo[*c*]chrysene is similar to that of N[1,2-*a*]P. On the basis of our results and those reported in the literature, our working hypothesis is that N[1,2-*a*]P may be added to the list of potent carcinogens that includes DB[*a,l*]P; this hypothesis is currently being tested in our laboratory.

Acknowledgment. This study was supported by NCI Contract NCI-CB-77022-75 and Cancer Center Support Grant CA-17613. We thank Ms. Ilse Hoffmann for editing the manuscript. The research described in this article has been reviewed by the National Health and Environmental Effects Research Laboratory, U.S. Environmental Protection Agency, and approved for publication. Approval does not signify that the contents necessarily reflect the views of the Agency nor does mention of trade names or commercial products constitute endorsement or recommendation for use.

References

(1) Cavalieri, E. L., Higginbotham, S., RamaKrishna, N. V. S., Devanesan, P. D., Todorovic, R., Rogan, E. G., and Salmasi, S. (1991) Comparative dose−response tumorigenicity studies of dibenzo[*a,l*]pyrene versus 7,12-dimethylbenz[*a*]anthracene, benzo[*a*]pyrene, and two dibenzo[*a,l*]pyrene dihydrodiols in mouse skin and rat mammary gland. *Carcinogenesis* **12**, 1939−1944.

(2) Cavalieri, E. L., Rogan, E. G., Higginbotham, S., Cremonesi, P., and Salmasi, S. (1989) Tumor-initiating activity in mouse skin and carcinogenicity in rat mammary gland of dibenzo[*a,l*]-pyrenes: the very potent environmental carcinogen dibenzo[*a,l*]-pyrene. *J. Cancer Res. Clin. Oncol.* **115**, 67−72.

(3) Durant, J. L., Busby, W. F., Lafleur, A. L., Penman, B. W., and Crespi, C. L. (1996) Human cell mutagenicity of oxygenated, nitrated and unsubstituted polycyclic aromatic hydrocarbons associated with urban aerosols. *Mutat. Res.* **371**, 123−175.

(4) Higginbotham, S., RamaKrishna, N. V. S., Johansson, S. L., Rogan, E. G., and Cavalieri, E. L. (1993) Tumor-initiating activity and carcinogenicity of dibenzo[*a,l*]pyrene versus 7,12-dimethylbenz[*a*]anthracene and benzo[*a*]pyrene at low doses in mouse skin. *Carcinogenesis* **14**, 875−878.

(5) Busby, W. F., Smith, H., Crespi, C. L., and Penman, B. W. (1995) Mutagenicity of benzo[*a*]pyrene and dibenzopyrenes in the *Salmonella* typhimurium TM677 and the MCL-5 human cell forward mutation assays. *Mutat. Res. Gen. Toxicol.* **342**, 9−16.

(6) Harvey, R. G. (1991) *Polycyclic aromatic hydrocarbons: chemistry and carcinogenicity*, 192 p, Cambridge University Press, Cambridge, U.K.

(7) Lacassagne, A., Buu-Hoi, N. P., and Zajdela, F. (1960) Activite cancerogene d'hydrocarbures polycycliques derives du naphthacene. *C. R. Acad. Sci.* **250**, 3547−3548.

(8) Dipple, A., Moschel, R. C., and Bigger, C. A. H. (1984) Polycyclic Aromatic Hydrocarbons. In *Chemical Carcinogens* (Searle, C. E., Ed.) ACS Monograph 182, American Chemical Society, Washington, DC.

(9) Dipple, A., Pigott, M. A., Agarwal, S. K., Yagi, H., Sayer, J. M., and Jerina, D. M. (1987) Optically active benzo[*c*]phenanthrene diol epoxides bind extensively to adenine in DNA. *Nature* **327**, 535−536.

(10) Cheng, S. C., Hilton, B. D., Roman, J. M., and Dipple, A. (1989) DNA adducts from carcinogenic and noncarcinogenic enantiomers of benzo[*a*]pyrene dihydrodiol epoxide. *Chem. Res. Toxicol.* **2**, 334−340.

(11) Lin, J.-M., Desai, D., Chung, L., Hecht, S. S., and Amin, S. (1999) Synthesis of anti-7,8-dihydroxy-9,10-epoxy-7,8,9,10-tetrahydro-

11-methylbenzo[*a*]pyrene and its reaction with DNA. *Chem. Res. Toxicol.* **12**, 341−346.

(12) Rice, J. E., and Cai, Z.-W. (1993) An intramolecular arene triflate coupling reaction for the regiospecific syntheses of substituted benzofluoranthene. *J. Org. Chem.* **58**, 1415−1424.

(13) Desai, D. H., Krzeminski, J., Lin, J.-M., and Amin, S. (2000) Syntheses and identification of 5-methylbenzo[*c*]chrysene metabolites. *Proceedings of the 91st Annual Meeting of the American Association of Cancer Research*, p 572, Abstract 3646, San Francisco, CA.

(14) Harvey, R. G. (1997) *Polycyclic Aromatic Hydrocarbons*, 232 pp, Wiley-VCH, New York.

(15) Zinke, A., Zimmer, W., Ott, R., and Wiesenberger, E. (1951) On the construction of benzpyrenes from chrysene. Report II: about 1,2,4,5-dibenzpyrene. *Monatsh. Chem.* **82**, 348−358.

(16) Desai, D., Krzeminski, J., Lin, J.-M., Chaddha, A., Miyata, N., Yagi, H., Jerina, D. M., and Amin, S. (1999) Synthesis and identification of benzo[*c*]chrysene metabolites. *Polycyclic Arom. Compd.* **16**, 255−264.

(17) Maron, D. M., and Ames, B. N. (1983) Revised methods for the *Salmonella* mutagenicity test. *Mutat. Res.* **113**, 173−215.

(18) Reznikoff, C. A., Brankow, D. W., and Heidelberger, C. (1973) Establishment and characterization of a cloned line of C3H mouse embryo cells sensitive to post confluence inhibition of division. *Cancer Res.* **33**, 3231−3238.

(19) Mohapatra, N., MacNair, P., Bryant, B. J., Ellis, S., Rudo, K., Sangaiah, R., Gold, A., and Nesnow, S. (1987) Morphological transforming activity and metabolism of cyclopenta-fused isomers of benz[*a*]anthracene in mammalian cells. *Mutat. Res.* **188**, 323−334.

(20) Reznikoff, C. A., Bertram, J. S., Brankow, D. W., and Heidelberger, C. (1973) Quantitative and qualitative studies of chemical transformation of cloned C3H mouse embryo cells sensitive to post confluence inhibition of cell division. *Cancer Res.* **33**, 3239−3249.

(21) Baird, W. M., and Brookes, P. (1973) Isolation of the hydrocarbon-deoxyribonucleoside products from the DNA of mouse embryo cells treated in culture with 7-methylbenz[*a*]anthracene-^{3}H. *Cancer Res.* **33**, 2378−2385.

(22) Kumar, S. (2001) A convenient and general synthesis of *cata*- and *peri*-condensed polycyclic aromatic hydrocarbons with a fjord-region. *Synthesis*, 841−844.

(23) Kumar, S. (1998) A new efficient route of the phenolic derivatives of chrysene and 5-methylchrysene, precursors to dihydrodiol and diol epoxide metabolites of chrysene and 5-methylchrysene, through Suzuki cross-coupling reaction, *J. Chem. Soc., Perkin Trans. 1*, 3157−3161.

(24) Zhang, F. L., Cortez, C., and Harvey, R. G. (2000) New synthetic approach to polycyclic aromatic hydrocarbons and their carcinogenic metabolites: Derivatives of benzo[*s*]picene, benzo[*rst*]pentaphene, and dibenzo[*b,def*]chrysene. *J. Org. Chem.* **65**, 3952−3960.

(25) Sharma, A. K., Kumar, S., and Amin, S. (2002) An abbreviated synthesis of 7,12-dimethylbenz[*a*]anthracene and benzo[*c*]chrysene metabolites using the Suzuki reaction. *Polycyclic Aromat. Compd.* (in press).

(26) Wislocki, P., Wood, A. W., Chang, R. L., Levin, W., Yagi, H., Hernandez, O., Dansette, P. M., Jerina, D. M., and Conney, A. H. (1976) Mutagenicity and cytotoxicity of benzo[*a*]pyrene arene oxides, phenols, quinones, and dihydrodiols in bacterial and mammalian cells. *Cancer Res.* **36**, 3350−3357.

(27) Nesnow, S., Davis, C., Nelson, G., Ross, J. A., Allison, J., Adams, L., and King, L. C. (1997) Comparison of the morphological transforming activities of dibenzo[*a,l*]pyrene and benzo[*a*]pyrene in C3H10T1/2CL8 cells and characterization of the dibenzo[*a,l*]-pyrene-DNA adducts. *Carcinogenesis* **18**, 1973−1978.

(28) Ross, J. A., and Nesnow, S. (1999) Polycyclic aromatic hydrocarbons: correlations between DNA adducts and *ras* oncogene mutations. *Mutat. Res.* **424**, 155−166

(29) Lin, J.-M., Boyiri, T., Krzeminski, J., Desai, D., El-Bayoumy, K., and Amin, S. (2001) Comparative mammary carcinogenicity in the rat and in vitro DNA adduct formation of bay-and fjord-region diol epoxides of benzo[*c*]chrysene (manuscript in preparation).

TX0200111